

# **LINER-LESS TANKS FOR SPACE APPLICATION – DESIGN AND MANUFACTURING CONSIDERATIONS**

Brian H. Jones, Ph.D., bhjones@kaisercompositetek.com  
Min-Chung Li, Ph.D., mcli@kaisercompositetek.com  
Kaiser Compositetek Inc., 1095 Columbia St., Brea, CA 92821  
(714) 990-6300

## **ABSTRACT**

Composite pressure vessels, used extensively for gas and fuel containment in space vehicles, are generally constructed with a metallic liner, while the fiber reinforcement carries the major portion of the pressure-induced load. The design is dominated by the liner's low strain at yield since the reinforcing fibers cannot operate at their potential load-bearing capability without resorting to pre-stressing (or autofretting). An ultra high-efficiency pressure vessel, which operates at the optimum strain capability of the fibers, can be potentially achieved with a "liner-less" construction. This paper discusses the design and manufacturing challenges to be overcome in the development of such a pressure vessel. These include: (1) gas/liquid containment and permeation, (2) design and structural analysis, and (3) manufacturing process development. The paper also presents the development and validation tests on a liner-less pressure vessel developed by Kaiser Compositetek Inc. (KCI). It should be noted that KCI's liner-less tank exhibits a highly controlled leak-before-burst mode. This feature results in a structure having the highest level of safety.

## **1. INTRODUCTION**

Many pressurized tanks utilized in space applications typically use a metal liner reinforced with a high-performance filamentary composite material such as carbon, graphite, aramid and glass. If tank structural efficiency is to be maximized, it is necessary to operate at strains that may be of the order of 1%, assuming, say, a safety factor of 1.5. This is particularly desirable if carbon filaments are used, as they typically exhibit endurance limits that may be 75% to 80% of ultimate. Table 1 describes typical carbon fibers widely used in the manufacturing of filament-wound pressure vessels. The design efficiency of filament-wound, metal-lined, pressure vessels is controlled by the behavior of the liner while the efficiency of a similar plastic lined vessel is influenced by the parasitic weight of the liner.(1) In contrast, an ultra high-efficiency pressure vessel can be potentially achieved if a "liner-less" construction is employed. For a design of this type, a number of advantages immediately accrue. First, removing the liner and replacing it with a material having generally higher specific strength and stiffness, results in a lower weight tank. Second, removing the need for strain compatibility between the liner and the composite over-wrap permits a design to be achieved that is controlled by the behavior of the reinforcing fiber, resulting in a structure having inherently superior fatigue performance. Third, the tank will generally be of lower cost, since the metal liner typically dominates the overall cost of the vessel. However, a linerless tank presents a number of design and manufacturing challenges, including gas (or liquid permeation) and the need to create a means to wind the pressure vessel in the absence of the liner. Micro-cracking that occurs in the composite matrix due to transverse straining compounds the challenge of containing gas or liquid.(1) These issues are discussed in what follows. Afterwards, development and validation tests of KCI's liner-less tanks will be presented.

## **2. GAS PERMEATION AND CONTAINMENT**

In producing a liner-less tank, two immediate design issues relating to gas containment must be addressed. The first relates to the fact that the composite laminate is subjected to bi-directional stresses which will result in transverse micro-cracking at levels of strain significantly below the strain to failure along the fiber. The second is the fact that all polymers are gas permeable to varying degrees.

**2.1 Transverse Micro-Cracks** Since a pressure vessel may be considered as being in a state of in-plane biaxial strain, high strains in the direction of the filaments will be associated with comparable strains in the transverse direction. Because transverse failure strains caused by matrix cracks occur at about 0.5%, it is evident that in a design based upon "large" strains of the order of 1% along the filament direction will result in transverse "micro-

cracks”. The obvious effect of these micro-cracks is to provide a leakage path for the contained gas (or liquid) from the interior. Therefore, it is necessary to prevent the gas from leaking through the over-wrapped composite of the pressure vessel. A further concern is to prevent moisture entering the micro-cracks produced on the exterior of the vessel. If freezing of the moisture occurs; it can result in progressive damage to the composite laminate. The solution to these problems is to apply appropriately compliant coatings on the interior and exterior surface of the vessel capable of containing the micro-cracks.

Table 1: Carbon fibers, which are widely used to produce filament-wound pressure vessels

Fiber	Modulus (MPa)	Ultimate Strain (%)	Endurance Limit (e.g. 80% of Ultimate)	Operating Stain with a Safety Factor of 1.5
Toray T-1000GB, 12K	296,010	2.1	1.68	1.12
Toray T-800, 12K	296,010	1.8	1.44	0.96
Toray T-700, 24K	231,840	2.1	1.68	1.12
Herculus, IM7, 12K	276,000	1.8	1.44	0.96
Mitsubishi, Grafil MR50, 12K	285,660	1.9	1.52	1.01

**2.2 Polymeric Coating Material Selection** An extensive literature survey was conducted into the use of various polymer and elastomer films and coatings to decrease the permeation of gases such as helium, hydrogen and oxygen through composite laminates. Figure 1 summarizes the helium permeability of some polymers and elastomers as the result of the literature search. Among them, ethylene vinyl alcohol (EVOH) and vinylidene chloride (PVDC) are superb barriers against the permeation of helium. On the other hand, fluoropolymers have very high permeability against helium. Among the elastomers found in the literature, polysulfide, polyurethane, nitrile and butyl have very low permeability. However, silicone and neoprene are very poor barrier materials.

ASTM 1434 test method was utilized to characterize the permeability of composite laminates containing EVOH films. Table 2 shows the laminate architecture of the test coupons. Figure 2 shows details of the permeation test setup. The test cell consists of a stainless steel chamber, closed by a three-inch diameter diaphragm made from the composite laminate under evaluation. The chamber is pressurized with either helium or oxygen. Pressure fluctuation was observed through a transducer that is accurate to  $\pm 1$  psi. or a digital pressure gauge that is sensitive to  $\pm 0.25$  psi. and accurate to  $\pm 1.25$  psi. Additionally, a dial gauge monitored the diaphragm deflection under pressure when required. A major challenge of the permeation test is sealing of the diaphragm to the gas filled chamber. It is achieved with a lead annular gasket, a butyl O-ring and a torque of 25 to 30 ft.-lbs. on the bolts used to clamp the upper and lower sections of the test chamber.

Table 2: Permeability test coupon laminate architecture, cure condition and gas with which the test is conducted

Reference	Lay-up	Thickness (in.)	Notes
1	90/0 <sub>2</sub> /90/FM300/0 <sub>2</sub> /FM300/EVOH/FM300	0.043	T700/epoxy laminate, vacuum bagged and oven cured, tested with helium
2	90/0 <sub>2</sub> /90/FM300/0 <sub>2</sub> /FM300/EVOH/FM300	0.043	T700/epoxy laminate, vacuum bagged and oven cured, tested with oxygen
3	FM300/EVOH/0/90/0/EVOH	0.052	T1000/epoxy filament-wound laminate, autoclave cured, tested with helium

Pressurization was accomplished using a container of pressurized gas regulated to the required level (100 psig. to 400 psig.). For tests carried out at elevated and cold temperatures, the test cell was placed into an environmental chamber that was maintained at the required temperatures.

Test results are shown in Figures 3 to 5 in the form of pressure and temperature histories. Figure 3 exhibits the temperature and helium pressure history of coupon 1 in Table 2 at ambient temperature, -100°F and 140°F. As noted, the pressure drops by about 20 psig. in 6 days. For the same laminate architecture tested with oxygen at the same pressure, no indication of pressure decrease was observed, as shown in Figure 4. Figure 5 shows helium pressure and temperature histories of coupon 3 in Table 2. There is no evidence of pressure drop for an autoclave-

cured laminate. Although leaking through gaskets, O-rings and fittings might be a concern and laminate architectures are not quite the same between the coupons tested, it is believed, predictably, that autoclave-cured laminate provide better structural integrity than those that were vacuumed-bagged and oven-cured. It is also shown that EVOH has very good permeability properties when the substrate laminate is autoclave-cured.

### 3. MANUFACTURING PROCESS DEVELOPMENT AND STRUCTURAL ANALYSIS

The design of a liner-less tank involves particular attention to features that are somewhat unique to this type of construction. They include end-fitting design, ratio of fitting size to the tank size and the impact of the tank aspect ratio on the tank efficiency factor (PV/W). These subjects were discussed in great detail in Reference 1. What follows discusses topics involving manufacturing process development and structural analysis.

**3.1 Manufacturing Process Development** To fabricate a liner-less pressure vessel, the reinforcing fibers must be wound onto a mandrel that is either water soluble, collapsible, or otherwise removable. The applicability of each concept will be dependent upon the physical size of the vessel and also the size of the opening. If the fitting size at the dome ends is small, water-soluble and collapsible tooling may not be feasible. The presence of permeation barrier films, coatings etc. on the interior surface will also limit the type of mandrel that is suitable. KCI's patented design of the liner-less pressure vessel evolves around a thin composite shell that is obtained by filament winding with a hard tooling. The hard tooling describes precisely the interior profile of the finished pressure vessel. After being cured in an autoclave, the structural composite shell is sectioned in half and taken off the tooling for preparation of joint, fitting installation and polymeric permeation coating application. Afterwards, the composite shell is joined together by bonding and the rest of composite, as required by design, will be wound on the composite shell to obtain the liner-less pressure vessel.

**3.2 Structural Analysis** Detailed 3-D finite element models were developed to design/analyze the composite laminate architectures of the liner-less pressure vessel. It should be noted that the geodesic filament-winding pattern results in a constant changing ply architecture (thickness and orientation) throughout the dome and particularly in the region of the fittings. As such, accurate modeling of the region is critical. A further challenge was created by the availability of data for composites and adhesives at the low operating temperatures required for the pressure vessels. Additionally, shear behavior of most epoxy adhesive is very non-linear.(2) For those adhesives which have their shear behavior characterized, data were usually available in a temperature range of -55°C (-67°F) and 82°C (180°F) from a single-lap shear test (ASTM D1002).(3) This is not a good indication of adhesive shear behavior due to the thin adherends (1.6 mm or 0.063 in.) used. During such a test, peel is inevitably induced across the adhesive bond line. Thus, indication of shear strength tends to be compromised. More accurate shear behavior could be obtained from a KGR-1 single-lap shear test with thick adherends. Therefore, the nonlinear behavior of the adhesive has to be accounted for in the design and analysis to obtain accurate analysis predictions.

### 4. DEVELOPMENT AND VALIDATION TESTS

Development and validation tests were conducted in sub-scale and full-size levels. Table 3 shows the specifications of the sub-scale and full-size H<sub>2</sub> and O<sub>2</sub> tanks. The sub-scale tank size is about one-third that of the full-size H<sub>2</sub> tank. Development and validation tests includes pressure proof and cycle tests at ambient and low temperatures, leak check at ambient temperature after the tanks went through each pressure test and hydraulic and pneumatic burst tests.

**4.1 Sub-Scale Tank Development Test** A sketch of the sub-scale tank test setup for proof and cycle tests is shown in Figure 6. To accommodate test temperatures down to -120°F, ethyl alcohol was used as the test media and an accumulator was installed between the pump and the tank outside of the test chamber to separate the ethanol and the hydraulic fluid. On one of the sub-scale tanks, strain gauges were installed to record the strains at various pressures. Data were compared with FEM predicted strain results. Leak checking was conducted after the tanks were subjected to the proof test or pressure cycle test to confirm that the permeation rate satisfied the requirements of Table 3.

Figures 7 to 8 are sample results of the sub-scale tank development tests. In Figure 7, reasonable agreement between strain gauge data and analytical prediction is observed. Figure 8 shows the temperature and pressure history of a helium leak check conducted after a sub-scale tank was subjected to a proof test of 1,015 psig. producing the same strain level in a full-size H<sub>2</sub> tank at its MEOP (400 psig.). Also shown in Figure 8 is the permeation or leak rate estimation of a full-size tank of the same laminate thickness from the leak check of the sub-scale tank. As seen in Figure 8, leak rate tested by helium easily satisfies the specification requirement.

Table 3: Sub-scale and full-size liner-less pressure vessel specifications

	Sub-scale Tank	H <sub>2</sub> Tank	O <sub>2</sub> Tank
OD (in.)	12.9	40.7	31.7
Length (in.)	22.5	55.1	41.7
Boss OD (in.)	2	2.375	2.375
Target Weight (lbs.)	9.1	31	16
Volume (in. <sup>3</sup> )	1,791	56,494	25,156
Aspect Ratio	1.74	1.35	1.32
MEOP (psig.)	1,000	400	400
Proof Pressure (psig.)	up to 1,100	440	440
Min. Burst Pressure (psig.)	1,500	600	600
Min. T (F)	-120	-120	-120
Max. T (F)		140	140
Tank Life to MEOP (cycles)	2,000	5,000	5,000

To obtain the failure mode of KCI's liner-less tanks, one sub-scale tank was subjected to pneumatic burst test. The tank exhibited a failure mode of leak-before-burst. The test result proved that the liner-less tank KCI designed has the highest level of safety due to the fact that there is no sudden and potentially unstable transfer of load between the composite structure and the metal liner when either one fails. Figure 9 show the sub-scale tank after the pneumatic burst test. The tank was apparently not ruptured and leaking was observed throughout the tank surface.

**4.2 Full-Size Ground-Test Tank Validation Test** Full-size ground-test H<sub>2</sub> and O<sub>2</sub> tanks were designed to have a safety factor three times of that of the H<sub>2</sub> and O<sub>2</sub> tanks specified in Table 3. The size of the full-size tanks prohibited the use of the in-house hydraulic pump for the pressure tests. Therefore, a test setup combining pneumatic and hydraulic means of pressurization was designed and assembled in house. A schematic diagram of the setup is shown in Figure 10. Both H<sub>2</sub> and O<sub>2</sub> ground-test tanks were subjected to proof test to 600 psig. and 2,000 cycles of pressurization test to 400 psig. at ambient temperature. Permeation test with helium was conducted after the proof and cycle tests. Results of the permeation test were shown in Figure 11. It can be seen that, after the proof test, practically no leak was detected. After cycle testing, however, some leakage or permeation was detected within the limits specified by the specifications.

## 5. SUMMARY

Composite pressure vessels, which have a metallic or a plastic liner, cannot achieve maximum efficiency because the liner does not have the same high specific stiffness, specific strength or strain capability as the composite over-wrap. An ultra high-efficient pressure vessel, which operates at a strain level of the order of 1%, can be achieved using a liner-less construction as proved by the sub-scale development tests described. Among the polymeric film and coating materials investigated, ethylene vinyl alcohol (EVOH) is a useful permeation barrier material. Autoclave-cured laminates have better structural integrity than vacuum-bagged, oven cured laminates and are the choice of substrate for polymeric coating materials. Furthermore, KCI's patented liner-less pressure vessel exhibits the highest level of safety with a benign failure mode of leak-before-burst.

## 6. ACKNOWLEDGEMENT

The work was partially sponsored by AeroVironment, Inc. in Simi Valley, California under funding from the NASA ERAST program.

## 7. REFERENCES

1. Li, Min-Chung and Jones, Brian H., "The Design of Composite Pressurized Tanks with and without Liners for Use in Space Applications", 33<sup>rd</sup> International SAMPE Technical Conference, Seattle, WA, Nov. 5-8, 2001
2. Heslehurst, R. B., SAMPE International Symposium 2001, 380 (2001).
3. American Society for Testing and Materials, "ASTM D1002-99, Standard Test Method for Strength Properties of Adhesives in Shear by Tension Loading (Metal-to-Metal)", ASTM, West Conshohocken, Pennsylvania, 1999.

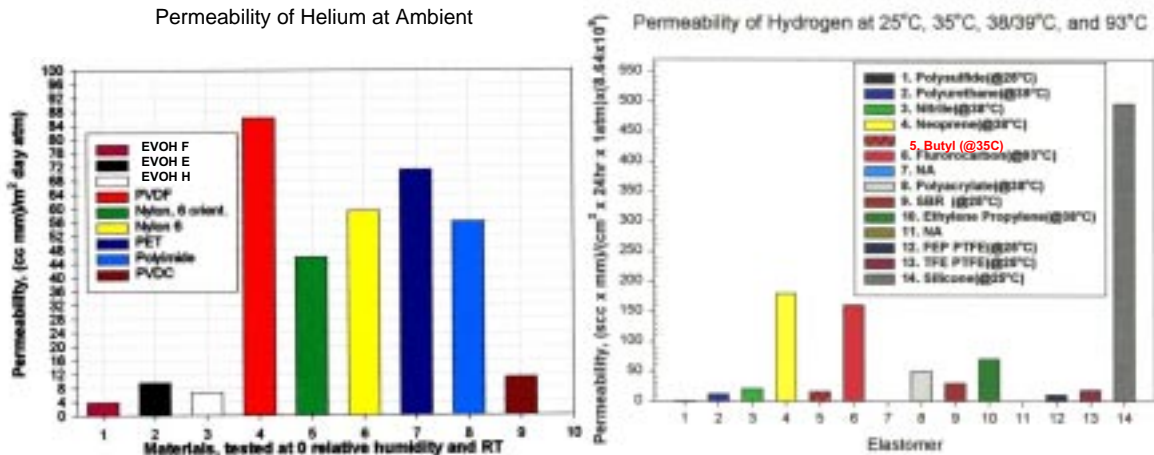


Figure 1: Helium and hydrogen permeability of various polymers and elastomers from literatures



Figure 2: Permeation test setup

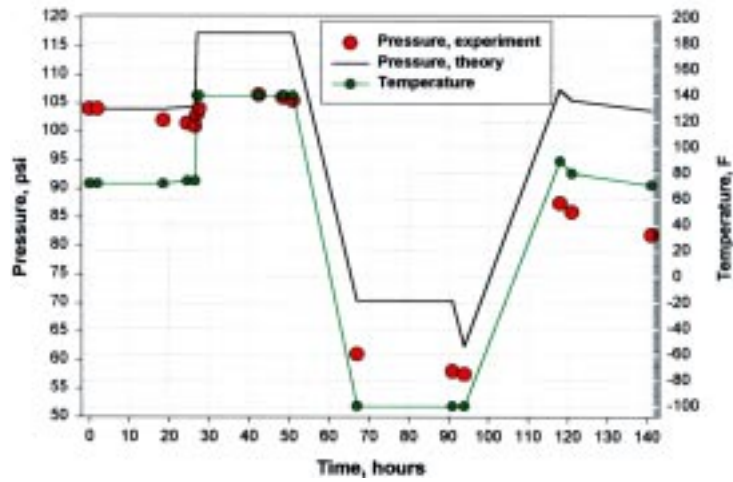


Figure 3: Pressure and temperature histories of coupon 1 of Table 2 from the permeation test

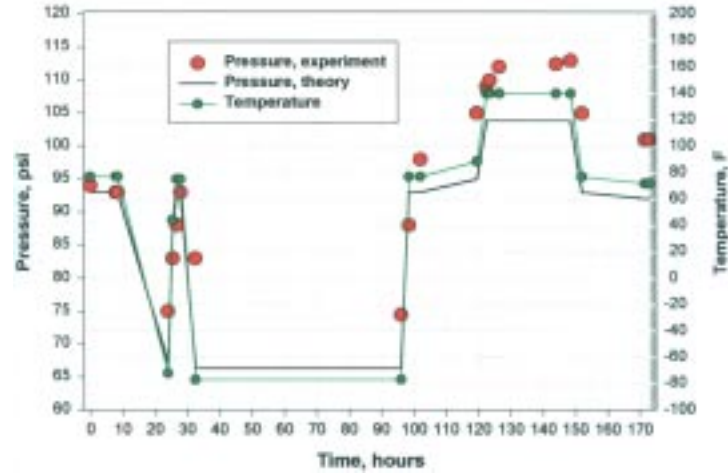


Figure 4: Pressure and temperature histories of coupon 2 of Table 2 from the permeation test

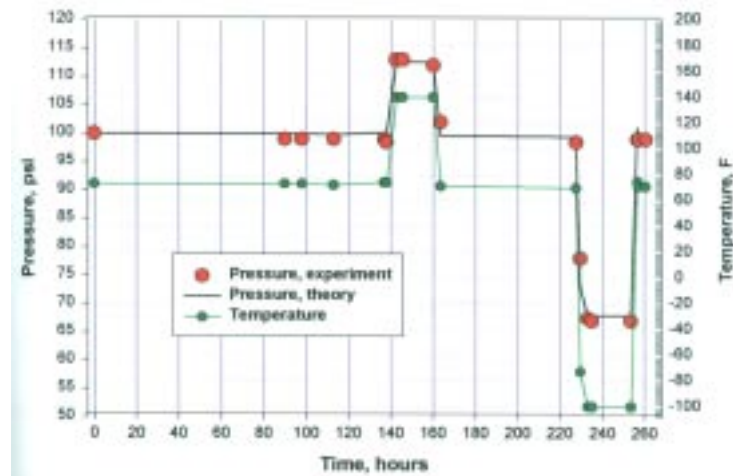


Figure 5: Pressure and temperature histories of coupon 3 of Table 2 from the permeation test

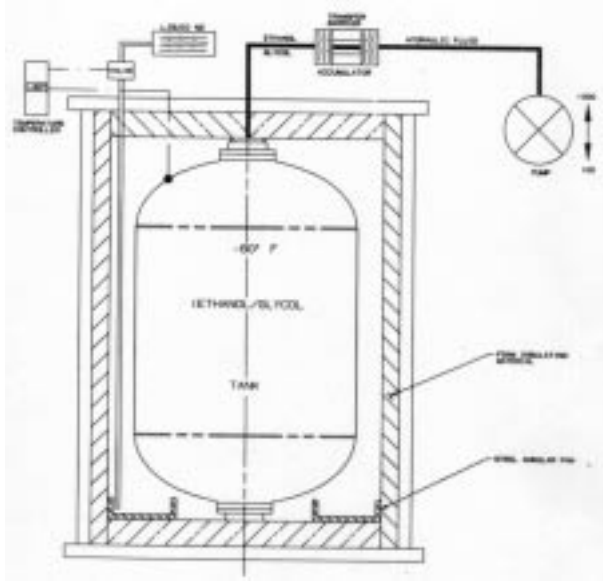


Figure 6: Pressure proof and cycle test setup for a sub-scale liner-less pressure vessel

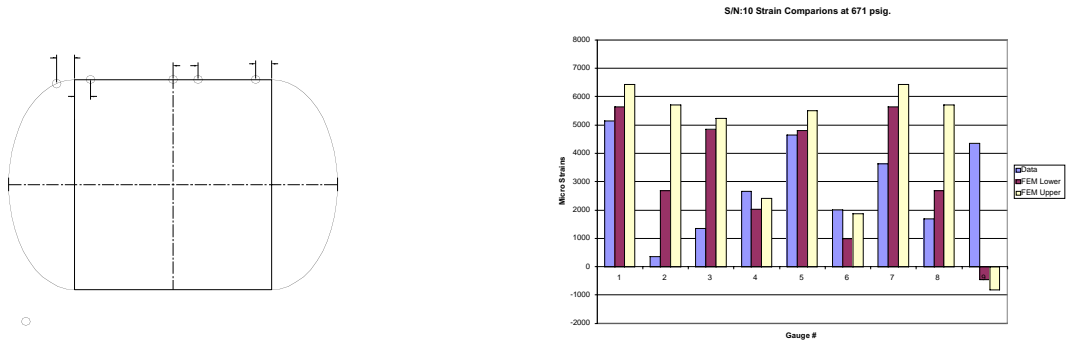
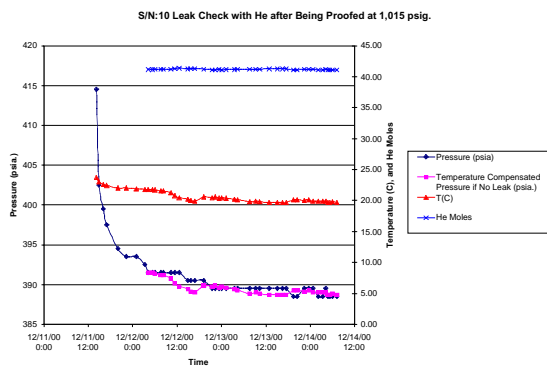


Figure 7: Strain gauge locations and strain data versus FEA results



S/N:10 Leak Check Summary and Full-Size H2 Tank Fuel Leak Rate Estimation			
Subscale Tank Test Summary	Full-size H2 Tank Leak Rate Estimation		
Volume (in. <sup>3</sup> )	2276	Volume	51,925
Surface Area (in. <sup>2</sup> )	848.6	Surface Area (in. <sup>2</sup> )	6,929.7
Initial Pressure (psia)	391.5	Allowable Leak Volume at -40F at 400 psig for 180 days (in. <sup>3</sup> )	2,596.3
Initial Temperature (F)	71.2	Allowable Leak Volume at RT at 1 atm (in. <sup>3</sup> ) for 180 days	96,207
Initial Moles of He	41.137	Estimated leak Volume at RT at 1atm for 180 days (in. <sup>3</sup> )	23,058
Final Pressure (psia)	388.5		
Final Temperature (F)	67.4		
Final Moles of He	41.117		
Moles of He Leaked	0.021		
Elapsed Time (day)	2.124		
Volume of He Leaked at 1atm (in. <sup>3</sup> ) at RT	31.350		

Figure 8: Helium leak check data and permeation/leak estimation of a sub-scale liner-less pressure vessel

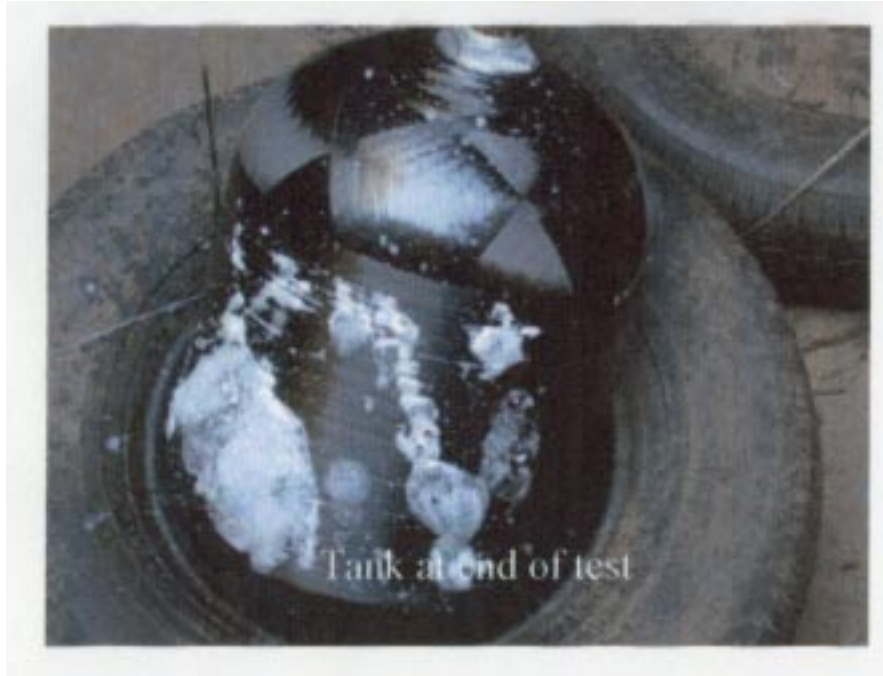


Figure 9: Leak-check on a liner-less tank after a pneumatic burst test shows an inert failure mode

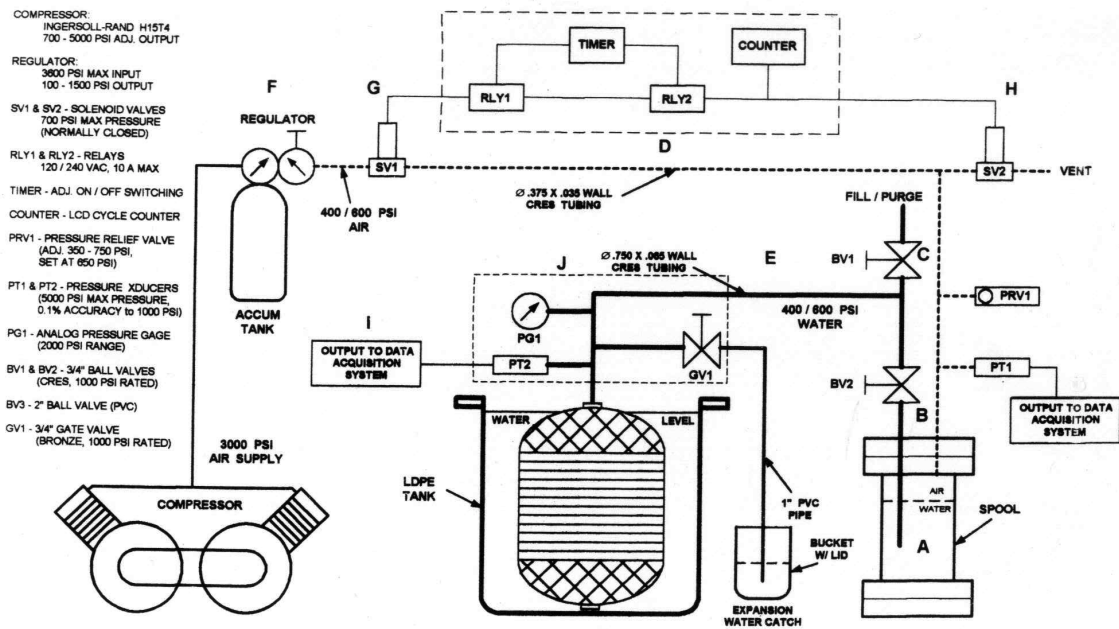


Figure 10: Full-size ground-test tank pressure proof and cycle test setup

H2 Ground Test S/N:1 He Leak Check after Proof to 600 psig. at RT			
Test Summary		Leak Rate Estimation	
Volume	56,494	Allowable Leak Volume at -40F at 400 psig for 180 days (in.^3)	2,824.7
Surface Area (in.^2)	7,371.2	Allowable Leak Volume at RT at 1 atm (in.^3) for 180 days	<b>103,274</b>
Initial Pressure (psia)	320.69	Estimated leak Volume at RT at 1atm for 180 days (in.^3)	<b>-336,846</b>
Initial Temperature (F)	81.01		
Initial Moles of He	821.22		
Final Pressure (psia)	325.82		
Final Temperature (F)	88.42		
Final Moles of He	823.10		
Moles of He Leaked	-1.877		
Elapsed Time (day)	1.94		
Volume of He Leaked at 1atm (in.^3) at RT	-2834.375		
O2 Ground Test S/N:1 1st He Leak Check after Proof to 600 psig. at RT			
Test Summary		Leak Rate Estimation	
Volume	25,156	Allowable Leak Volume at -40F at 400 psig for 180 days (in.^3)	1,257.8
Surface Area (in.^2)	4,274.5	Allowable Leak Volume at RT at 1 atm (in.^3) for 180 days	<b>45,986</b>
Initial Pressure (psia)	317.22	Estimated leak Volume at RT at 1atm for 180 days (in.^3)	<b>-367,619</b>
Initial Temperature (F)	80.19		
Initial Moles of He	362.27		
Final Pressure (psia)	322.89		
Final Temperature (F)	86.78		
Final Moles of He	364.30		
Moles of He Leaked	-2.028		
Elapsed Time (day)	1.94		
Volume of He Leaked at 1atm (in.^3) at RT	-3062.678		

H2 Ground Test S/N:1 He Leak Check after 2,000 Cycles to 400 psig. at RT			
Test Summary		Leak Rate Estimation	
Volume	56,494	Allowable Leak Volume at -40F at 400 psig for 180 days (in.^3)	2,824.7
Surface Area (in.^2)	7,371.2	Allowable Leak Volume at RT at 1 atm (in.^3) for 180 days	<b>103,274</b>
Initial Pressure (psia)	399.07	Estimated leak Volume at RT at 1atm for 180 days (in.^3)	<b>20,437</b>
Initial Temperature (F)	71.87		
Initial Moles of He	1039.52		
Final Pressure (psia)	401.61		
Final Temperature (F)	75.33		
Final Moles of He	1039.38		
Moles of He Leaked	0.143		
Elapsed Time (day)	1.96		
Volume of He Leaked at 1atm (in.^3) at RT	215.259		
O2 Ground Test S/N:1 He Leak Check after 2,000 Cycles to 400 psig. at RT			
Test Summary		Leak Rate Estimation	
Volume	25,156	Allowable Leak Volume at -40F at 400 psig for 180 days (in.^3)	1,257.8
Surface Area (in.^2)	4,274.5	Allowable Leak Volume at RT at 1 atm (in.^3) for 180 days	<b>45,986</b>
Initial Pressure (psia)	410.99	Estimated leak Volume at RT at 1atm for 180 days (in.^3)	<b>2,050</b>
Initial Temperature (F)	68.10		
Initial Moles of He	480.12		
Final Pressure (psia)	417.37		
Final Temperature (F)	76.31		
Final Moles of He	480.11		
Moles of He Leaked	0.015		
Elapsed Time (day)	2.01		
Volume of He Leaked at 1atm (in.^3) at RT	22.915		

Figure 11: Helium permeation/leak check result of full-size ground-test tanks before and after a pressure cycle test